International Journal of Microwave and Wireless Technologies, 2016, 8(6), 855–863.
doi:10.1017/S1759078716000593

RESEARCH PAPER

High-resolution signal processing techniques for through-the-wall imaging radar systems

AHMET SERDAR TURK[1], PINAR OZKAN-BAKBAK[1], LUTFIYE DURAK-ATA[2], MELEK ORHAN[1] AND MEHMET UNAL[1]

Through-the-Wall Imaging is an ever-expanding area in which processing time, scanning time, vertical, and horizontal resolutions have been tried to improve. In this study, several methods are investigated to obtain efficient reconstruction of through-the-wall imaging radar signals with high resolution. Microwave radar signals, which are produced in YTU Microwave Laboratory, are processed by compressive sensing (CS). B and C scanned reflection data samples collected between 1 and 7 GHz frequency band are taken randomly at 1/4, 1/2 of whole amount and reconstructed by CS method. Considering the signal structure, 10 and 20 compressible Fourier coefficients are taken through CS to analyze the difference between them. In addition, we applied synthetic aperture radar (SAR) processing, also combined with SAR-Multiple Signal Classification over raw data. Experimental performance results are given and shown in the figures with high quality.

Keywords: Compressive sensing, Ground penetrating radar, Through-the-wall imaging, Synthetic aperture radar, Multiple signal classification, Stepped frequency radar

Received 1 November 2015; Revised 24 March 2016; Accepted 3 April 2016; first published online 29 April 2016

I. INTRODUCTION

In the last decades, ground-penetrating radar (GPR) has become a leading technology for the detection, identification, and imaging of subsurface artifacts, abnormalities, and structures. It has a very broad range of applications [1–3]. GPR performance is associated with the electrical and magnetic properties of local soil and buried targets, as well as with implementation of the GPR hardware and software. The central frequency and bandwidth of the GPR signal chosen are key factors in the detection of subsurface features. Conventional GPRs are usually designed for geophysical applications and use central frequencies below 1 GHz. The lower frequencies are preferred to detect something buried too deep, due to the dramatically increased attenuation versus frequency. Nevertheless, the higher frequencies are needed for better range resolution and detailed echoes to determine small objects. Thus, GPR systems that transmit ultra-wide band (UWB) impulse signals are proposed primarily to benefit from both low and high frequencies [4]. Stepped-frequency (SF) technique offers some benefits compared with time-domain GPR systems. Most important, SF-GPR has a distinct advantage over conventional impulse GPR, where there is no effective control of the source frequency spectrum. Apart from increased resolution and increased depth of penetration, the signal spectrum received by SF-GPR offers the advantage of reading the real and phase parts, which can be made use of in analyzing subtle and complex inhomogeneities [5].

Through Wall Imaging (TWI) radar systems with microwave techniques, which allow us to see through obstacles such as concrete, brick, and trees, is highly popular research subject for military and civilian applications [6]. For example, it could be used in hostage rescue and anti-terror missions, in detection and locating survivors trapped inside a burning building, or in areas, which have been plagued by natural disasters (e.g. earthquakes or avalanches). Moreover, as a military application, it allows law enforcement to get an accurate target localization and classification of people and detection of objects within the building in a hostage crisis. In TWI radar systems, the microwave signals, which are able to penetrate to opaque obstacle, are radiated to the obstacles via antennas and back-scattered fields from the target objects are collected. After that, the collected back-scattered data are processed with signal processing techniques to obtain the high resolution images of the concealed targets and objects behind the wall. Furthermore, in such an imaging system, it is very useful to operate in the ultra-wide band (UWB) or multi-band, because of efficient penetration to the concrete, brick or wood at low frequencies, and for high resolution by using high frequencies.

Super-resolution is very important for the signal processing of GPR to resolve closely buried targets. However, it is not easy to get high resolution as GPR signals are very weak and enveloped by the noise. The multiple signal classification (MUSIC) algorithm, which is well known for its super resolution capacity, has been implemented for signal and image processing of GPR. Therefore, we implemented super-resolution spectral

[1]Yildiz Technical University, Davutpasa Campus, 34220 Istanbul, Turkey. Phone: +90 212 383 58 80
[2]Istanbul Technical University, Ayazaga Campus, 34469 Istanbul, Turkey
Corresponding authors:
A. S. Turk and P. Ozkan-Bakbak
Email: {asturk,pozkan}@yildiz.edu.tr

estimation technique MUSIC algorithm to improve the resolution capacity. This technique deals with a signal processing method used to increase the vertical resolution of a radar image and to obtain a high-precision signal level [7].

Synthetic aperture radar (SAR) is a well-known technique, which uses signal processing to improve the resolution beyond the limitation of physical antenna aperture [8]. In SAR, forward motion of actual antenna is used to synthesize a very long antenna. SAR allows the possibility of using longer wavelengths and still achieving good resolution with antenna structures of reasonable size. SAR is very useful over a wide range of applications, including sea and ice monitoring, mining, oil pollution monitoring, oceanography, snow monitoring, classification of earth terrain, etc. [9]. Recently, UWB SAR has become a promising technology for TWI radar systems, as well [10].

Compressive sensing (CS) method shows that reconstruction of unknown signals, which have a sparse or compressible representation in a certain transformation domain, can be obtained from a small set of measurements as compared with conventional techniques. CS keeps the information about the related signal in a relatively small number of random measurements. Research on CS has been spreading various areas such as communications, remote sensing, radar, information theory, image processing [11–17].

CS application for GPR imaging problem was first demonstrated in [18]. In that work, the subsurface area was modeled that consisted of a small number of discrete point-like targets, and a dictionary of model data was generated for each possible discrete target point. The subsurface image was generated by solving a ℓ_1 minimization-based optimization problem with a decreased number of measurements. Later, these results were extended to the SF [19] and impulse GPR [20] cases. In [21], Yoon, et al. used CS for through-the-wall imaging using wide-band beam forming, where the unmeasured frequency points were reconstructed with CS and conventional wideband beam forming was applied on the reconstructed measurements.

In this study, an UWB SF-GPR system scenario is designed and realized by Anritsu vector network analyzer. The network analyzer sweeps a wide signal band between 1 and 7 GHz. The continuous SF method is applied. The UWB transmitter and receiver antenna designed for this system is the partial dielectric loaded TEM fed ridged horn [22].

II. DATA ACQUISITION AND TEST MEASUREMENT

In this work, CS algorithm and SAR, MUSIC algorithms for super resolution are applied to TWI radar.

The transmission coefficient S_{21} is measured by the network analyzer over the operational band. For B-scan image data, S_{21} must be dependent on time. Therefore, the inverse Fourier transform of S_{21} is applied to obtain matrix T.

$$T = F^{-1}\{S_{21}\}. \tag{1}$$

The mathematical representation of equation (1) is given as

$$T = \frac{1}{N}\sum_{n=0}^{N-1} S_{21} e^{\frac{-2\pi jkn}{N}}, \tag{2}$$

where, k represents the sampled points in the time domain, lower case n represents the sampled points in the frequency domain, and N is the number of sampled points.

The background signal can be considered as a calibration or reference signal for ameliorating the image of collected data. This signal consists of the direct pulse from transmitting and receiving antennas, ringing from the antennas, and clutter from other objects (not targets) that reflect the electromagnetic energy within the antenna beam width. The clutter can be minimized by using lower band radiator antennas. Nevertheless, this case will degrade the image resolution, which will cause hard-recognition of small buried objects. To reduce the clutter effect on B-scan plot, the reference signal is collected at the non-target position of the space [23]. If the transmission coefficient S_{21}, which depends on time is symbolized by T, then background removed A-scan signal is calculated as

$$T_B = \frac{1}{N}\sum_{i=1}^{N} T_i(x, y, z), \tag{3}$$

$$T_{BR}(z) = T(z) - T_B(z), \tag{4}$$

where, a_i is each A-scan data obtained from initial clear region and N is its number, a_B represents the non-target background signal (3) and a_{BR} corresponds to background removed A-scan signal (4).

Then, the absolute of background removed T matrix is plotted by command "surface" and B-scan image is obtained in (5).

$$B = |T|. \tag{5}$$

III. CS

CS method can be divided into two main sections as sensing with minimal samples and reconstruction by sparse or compressible approach. Let, x be N–length sparse signal in sparse domain, which can be expressed with K-basis vectors as:

$$x = \Psi s. \tag{6}$$

If m measurements are taken from random projections onto Φ, the projected signal can be expressed as:

$$y = \Phi x = \Phi\Psi s. \tag{7}$$

Let Φ and Ψ be the projection and the base matrices, respectively, and the sparsity pattern vector is possible by the following convex optimization

$$\min \left\| \overset{\Lambda}{s} \right\| \; subject \quad to \quad \Theta s \le y, \tag{8}$$

where $\Theta = \Phi\Psi$.

In general, the GPR signal is noisy. Thus, the compressive measurement y_i at the ith aperture position have the following form:

$$y_i = \Phi_i\Psi_i s + noise_i, \tag{9}$$

https://doi.org/10.1017/S1759078716000593 Published online by Cambridge University Press

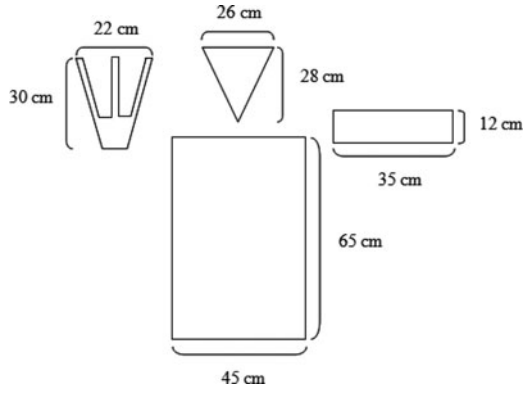

Fig. 1. Metal target model for TWI operation.

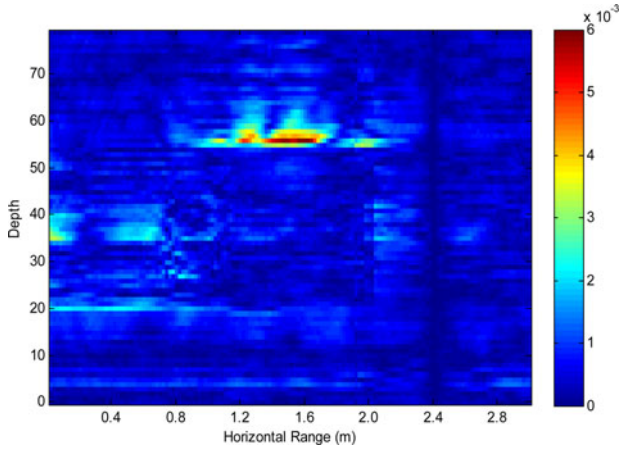

Fig. 2. B-scan measurement raw data (background removed).

and the convex optimization is supported by

$$\min \left\| \overset{\Lambda}{s} \right\| \; subject \quad to \quad \left| (\Theta \overset{\Lambda}{s} + noise) - \Theta s \right| \leq error. \qquad (10)$$

A convex optimization package is used for the numerical solution [24].

In this article, we use two scenarios for signal processing applications. The first scenario of our work is the investigation of body model behind a brick wall. Metal target model, which is used for through-wall imaging operation is shown in Fig. 1. The thickness of the wall is 30 cm. The distance from the antenna to the target is 85 cm. The wall is almost homogeneous and has bricks.

Figure 2 is the B-scan image of the original TWI radar background removed data; Fig. 3 is the CS results where 20 and 40 random measurements are taken, respectively, based on 10 Fourier compressible coefficients. In Fig. 4, 20 and 40 random measurements are taken, respectively, based on 20 Fourier compressible coefficients. In reconstruction process, the number of measurements is important. This issue determines the quality of the reconstructed signal. The other investigated case is Fourier coefficients, which are used to make the signal compressible. If the compressible coefficients, which construct the signal are decreased, the image resolution decreases. But, even if these coefficients are increased as enough, the quality of image resolution is acceptable as enough [22].

The second scenario is the model of two target objects as shown in Fig. 5. The thickness of the wall is 30 cm. The distances from the antenna to the targets are 1 and 1.5 m, respectively. The wall is almost homogeneous and has the bricks. The B-scan and C-scan images of raw data are given in Figs 6 and 7.

In Figs 8 and 9, noise reduction is observed by taking the top 10 sparse Fourier coefficients. % 50 random measurements are taken to get fine quality of image resolution in the results.

IV. SAR ALGORITHM

SAR algorithm is created by forming a fictional antenna array to obtain narrower beam in the area, organized by the footprint size of the radar. To obtain SAR beam of antenna at each scan point, as shown in Fig. 10, a balance phase term is added to S_{21} parameter depending on the distance from location of nth antenna to target point R_n given in (11)

$$R_n = \sqrt{H_T^2 + (nd)^2}, \qquad (11)$$

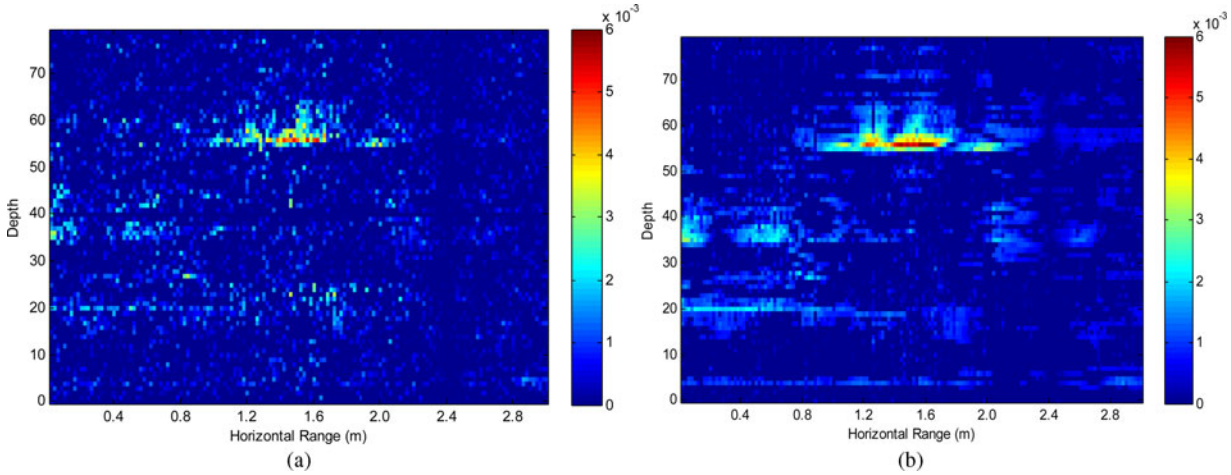

Fig. 3. (a) CS taken 20 random measurements based on 10 Fourier compressible coefficients (b) CS taken 40 random measurements based on 10 Fourier compressible coefficients.

https://doi.org/10.1017/S1759078716000593 Published online by Cambridge University Press

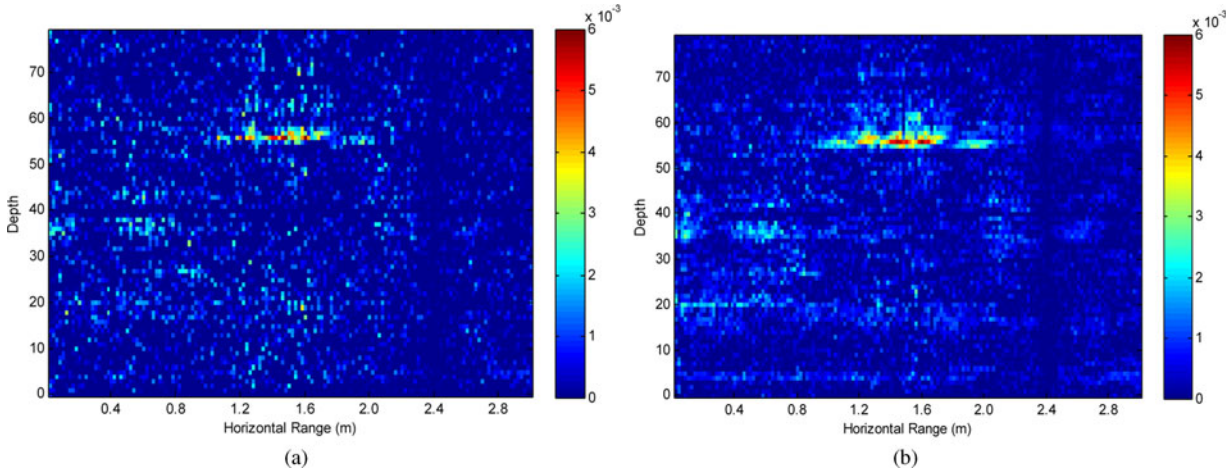

Fig. 4. (a) CS taken 20 random measurements based on 20 Fourier compressible coefficients (b) CS taken 40 random measurements based on 20 Fourier compressible coefficients.

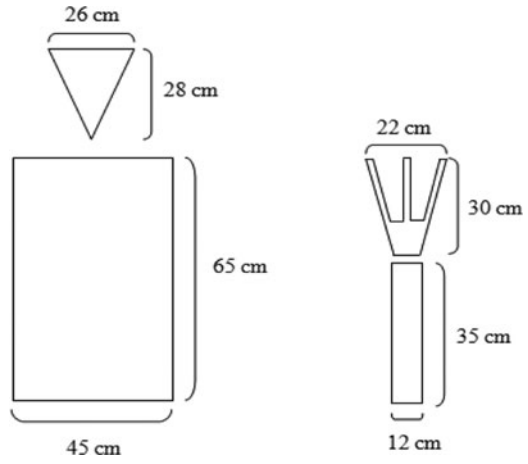

Fig. 5. Two metal target model for TWI operation (a) head and body, (b) arm and hand.

where, H_T and d are vertical distance from location of reference antenna to target point and distance between antennas, respectively. The illustration geometry for synthetic antenna array and difference between distances from location of each antenna to the target point is shown in Fig. 10.

The difference between distance from location of each antenna to target point and distance from location of the reference antenna to the target point,ΔR_n, is given in (12) as

$$\Delta R_n = R_n - H_T. \tag{12}$$

Then, SAR effect to S parameter, S_{21SAR} can be calculated as in (13)

$$S_{21SAR} = \sum_{n=1}^{N} S_{21} e^{jk\Delta R_n}, \tag{13}$$

where, k and N are the wave number and the number of antennas, respectively.

While a balance phase term is added to S_{21SAR} parameter, the angle between the distance from nth antenna to target and distance from reference antenna to target is calculated

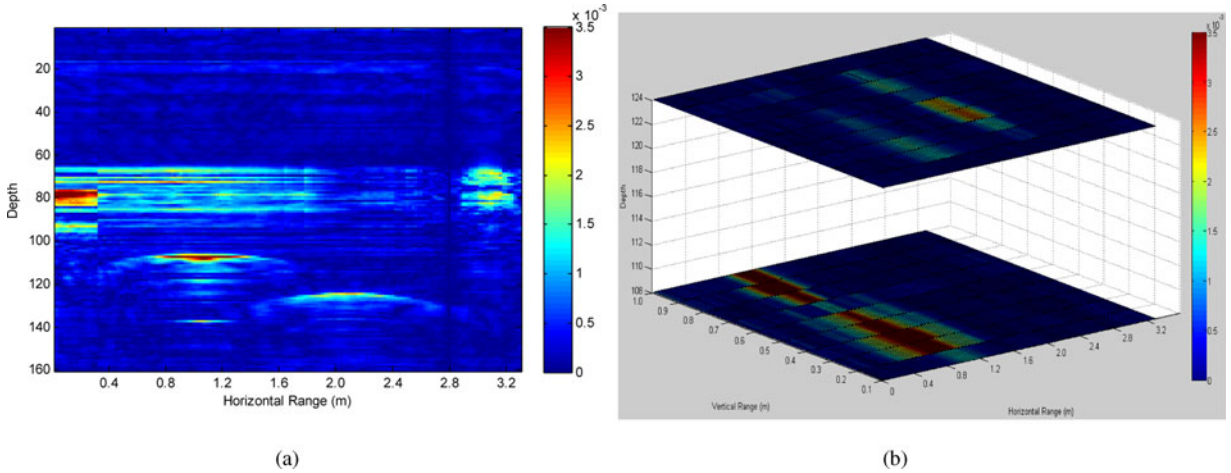

Fig. 6. Background removed raw data (a) B-scan, (b) C-scan.

https://doi.org/10.1017/S1759078716000593 Published online by Cambridge University Press

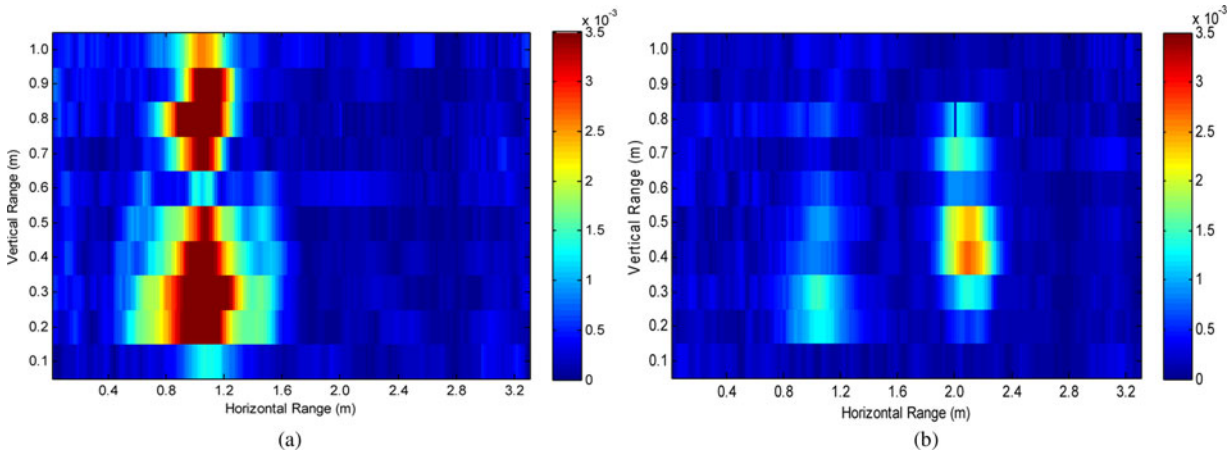

Fig. 7. Background removed raw data C-scan slices (a) head and body, (b) arm and hand.

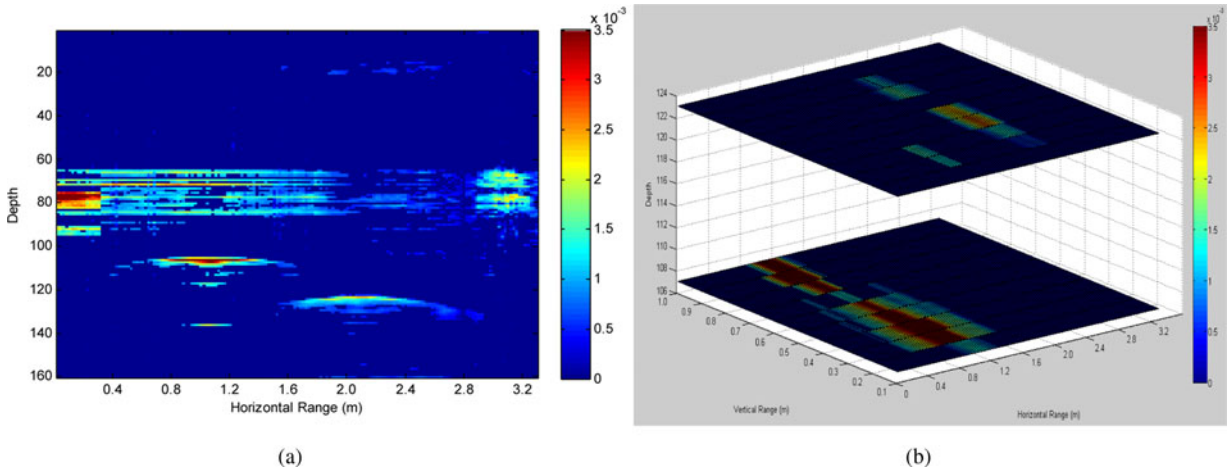

Fig. 8. CS taken 80 random measurements (%50 of all) based on 10 Fourier compressible coefficients (a) B-scan, (b) C-scan.

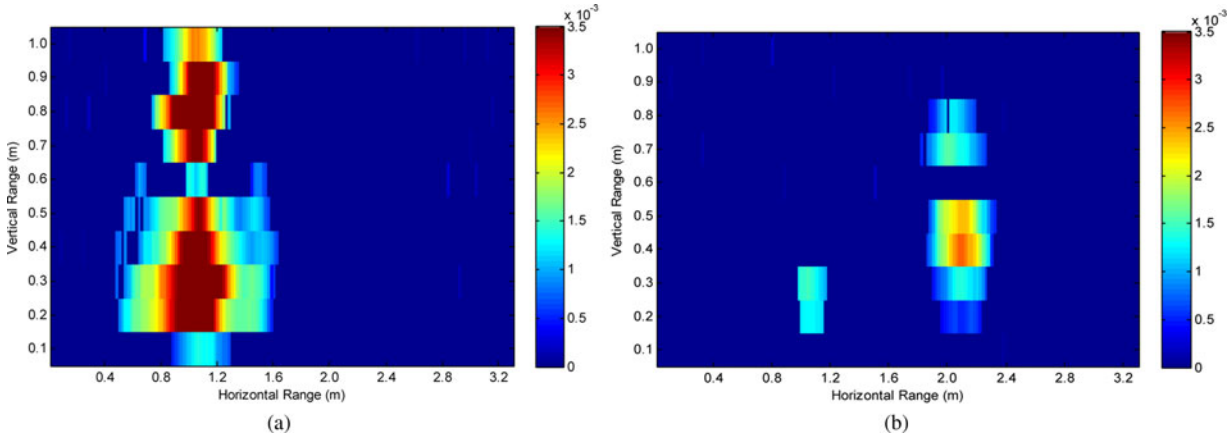

Fig. 9. C-scan CS images (a) head and body, (b) arm and hand.

as follows (14)

$$\tan\theta = \frac{nd}{H_T}. \tag{14}$$

Thereby, it was determined that the angle of the incoming signal (θ) can be associated with the antenna beam.

$$\theta = \tan^{-1}\left(\frac{nd}{H_T}.\frac{180}{\pi}\right). \tag{15}$$

https://doi.org/10.1017/S1759078716000593 Published online by Cambridge University Press

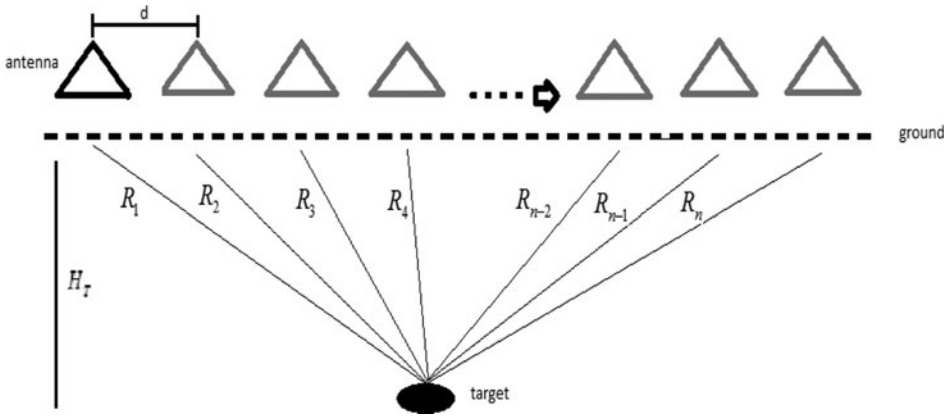

Fig. 10. Operating principle of fictive antenna array on SAR progress.

Also, SAR length of this process is calculated as given in (16)

$$L_{SAR} = Nd.$$

The SAR application of our work is investigation of two metal targets behind the brick wall.

The B-scan and C-scan slice of through-wall imaging SAR operation are given in Figs 11 and 12. It is seen that through-wall imaging SAR operation gives better horizontal resolution than the conventional GPR operation.

V. MUSIC ALGORITHM

The MUSIC algorithm is a nonparametric spectral estimation technique, which estimates multiple scattering centers from

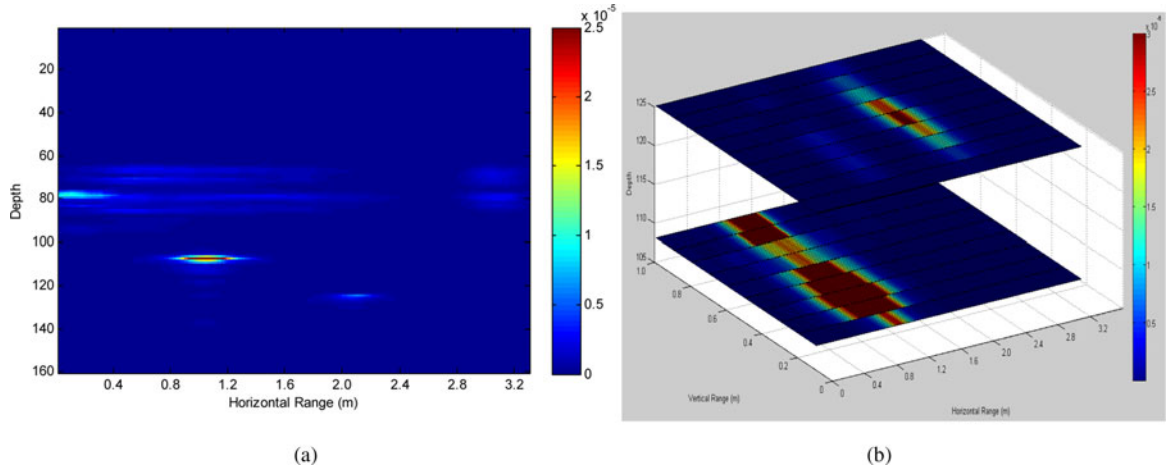

Fig. 11. (a) B-scan SAR data, (b) C-scan SAR image where targets on the slices.

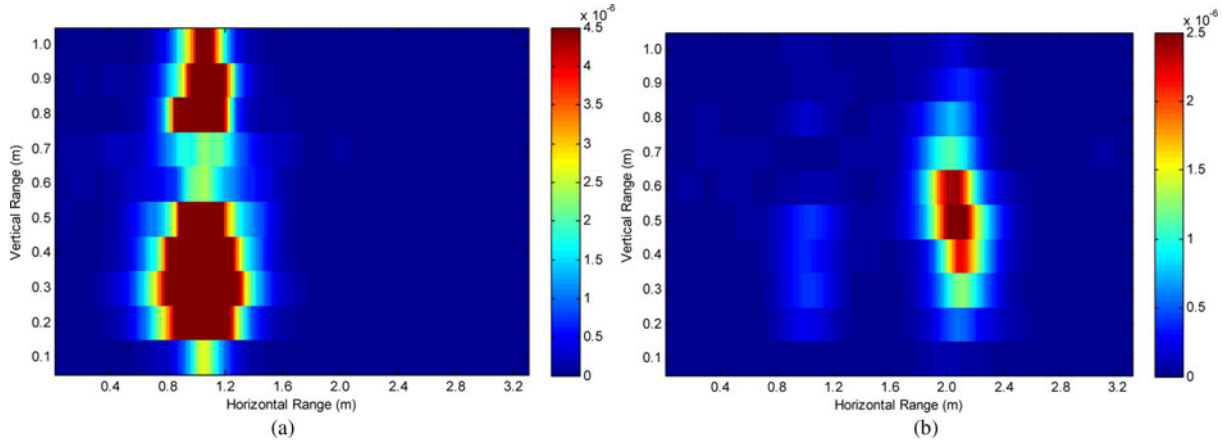

Fig. 12. C-scan slices of SAR algorithm result (a) head and body, (b) arm and hand.

https://doi.org/10.1017/S1759078716000593 Published online by Cambridge University Press

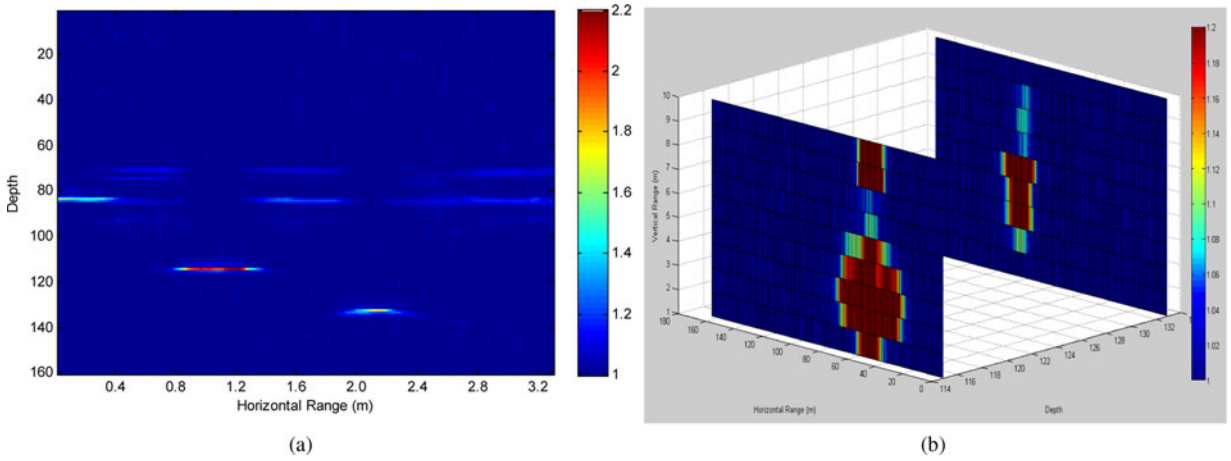

Fig. 13. Combined SAR and MUSIC algorithm result (a) B-scan, (b) C-scan.

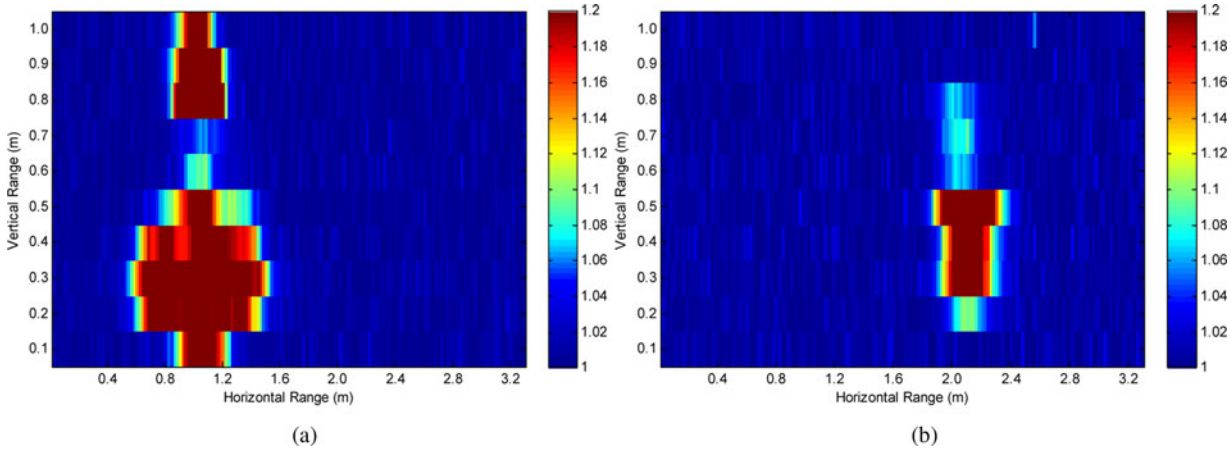

Fig. 14. C-scan slices of combined SAR and MUSIC algorithm (a) head and body, (b) arm and hand.

the observed voltage received on an array of antenna utilizing the eigenvector. The eigenvalue of diagonal matrix helps to estimate the numbers of reflected signals [7].

The signal covariance matrix of the transmission coefficient S_{21} is written as in (17)

$$C = S_{21}S_{21}^{*}, \tag{17}$$

where, * denotes complex conjugate transpose. Furthermore, incident wave and noise can be considered as not related (orthogonal). For this reason signal covariance matrix is divided into two orthogonal subspace matrixes. These spaces are called signal and noise subspace. This distinction is done with eigenvalue decomposition or singular value decomposition. v column vector of zero valued eigenvectors matrix is made up noise subspace of covariance matrix and is called projection matrix, P_{noise}.

If the point which is observed belongs to object, reaches to measuring point under a definite phase difference. Phase shift in frequency domain corresponds to time difference between two signals. If we consider the distance of x_i to antenna as d_i and is the velocity of wave propagation, delay time of signal which returns to receiver correspond to. If time intervals during the scanning is perpendicular to the noise subspace, it is called as scattering point.

$$a(\tau) = [e^{-2\pi f_1 \tau_L}, e^{-2\pi f_2 \tau_L}, \ldots, e^{-2\pi f_k \tau_L}], \tag{18}$$

where, $a(\tau)$ in (18) is a delay-time mode vector. It is calculated during the scan time (τ_L) and it depends on the number of frequency measurement, k.

The position (delay time) of each reflection point, P_{music} in (19), can be estimated by searching the peak position of the MUSIC function as [7]

$$P_{music}(\tau) = \frac{a(\tau)^{*}a(\tau)}{a(\tau)^{*}P_{noise}a(\tau)}. \tag{19}$$

In Figs 13 and 14, we propose a multi-processing approach, which combines SAR algorithm and time-domain response of MUSIC algorithm to obtain super-resolution in both horizontal and vertical scanning planes. In the case of real human target at similar sizes, the 1–7 GHz UWB signal-to-noise ratio performance of the figures could decrease up to 5 dB [25].

https://doi.org/10.1017/S1759078716000593 Published online by Cambridge University Press

VI. CONCLUSION

In this paper, using UWB partial dielectric loaded TEM horn antenna, through-the-wall imaging B and C-scan images are presented by CS, SAR and MUSIC. Reconstruction of the microwave radar signal is realized by CS with fewer and random measurements employing convex optimization. In reconstruction process, the number of measurements is important. This issue determines the quality of the reconstructed signal. The other investigated case is Fourier coefficients, which are used to make the signal compressible. If the compressible coefficients which construct the signal are decreased, the image resolution decreases. However, even if these coefficients are increased as enough, the quality of image resolution is acceptable as enough. On the second stage, the combination of SAR and MUSIC algorithms is employed to enhance the vertical and horizontal resolutions. Therefore, better detection of closely buried targets is possible with improved image quality.

ACKNOWLEDGEMENTS

Ahmet Serdar Turk and Mehmet Unal were supported by grant 110E222 of TUBITAK (The Scientific and Technological Research Council of Turkey) research fund.

REFERENCES

[1] Daniels, D.J.: Surface penetrating radar. IEE Radar, Sonar, Navigation and Avionics Series 6, IEE, London, 1996.

[2] Turk, A.S.; Hocaoğlu, A.K.: Buried object detection. Encyclopedia RF Microw. Eng., **1** (2005), 541–559.

[3] Borchert, O.; Aliman, M.; Glasmachers, A.: Directional borehole radar calibration. International Workshop on Advanced Ground Penetrating Radar, Italy, 2007.

[4] Sahinkaya, D.S.A.; Turk, A.S.: UWB GPR for detection and identification of buried small objects. Proc. SPIE, 2004.

[5] Kong, F.N.; By, T.L.: Theory and performance of a GPR system which uses step frequency signals. J. Appl. Geophys., **33** (1993), 453–445.

[6] Thajudeen, C.; Hoorfar, A.; Ahmad, F.: Measured complex permittivity of walls with different hydration levels and the effect on power estimation of TWRI target returns. Prog. Electromag. Res. B, **30** (2011), 177–199.

[7] Arai, L.; Shanker, M.S.: Signal processing of ground penetrating radar using spectral estimation techniques to estimate the position of buried targets. EURASIP J. Appl. Signal Process., **12** (2003), 1198–1209.

[8] Curlander, J.C.; McDounough, R.N.: Synthetic Aperture Radar, Systems and Signal Processing. John Wiley & Sons, New York, 1991.

[9] Chan, Y.K.; Koo, V.C.: An Introduction to synthetic aperture Radar (SAR). Prog. Electromag. Res. B, **2** (2008), 27–60.

[10] Dogaru, T.; Le, C.: Recent investigations in sensing through the wall radar modeling. Antennas and Propagation Society Int. Symp., 2008. AP-S 2008, IEEE, 5–11 July 2008, 1–4.

[11] Baraniuk, R.G.: Compressive sensing lecture notes. IEEE Signal Process. Mag., **24** (2007), 118–121.

[12] Candès, E.; Romberg, J.; Tao, T.: Robust uncertainty principles: exact signal reconstruction from highly incomplete frequency information. IEEE Trans. Inform. Theory, **52** (2006), 489–509.

[13] Candès, E.; Romberg, J.; Tao, T.: Stable signal recovery from incomplete and inaccurate measurements. Commun. Pure Appl. Math., **59** (2006), 1207–1223.

[14] Donohoo, D.: Compressed sensing. IEEE Trans. Info. Theory, **52** (2006), 1289–1306.

[15] Candès, E.; Tao, T.: Near optimal signal recovery from random projections and universal encoding strategies. IEEE Trans. Info. Theory, **52** (2006), 5406–5425.

[16] Candès, E.; Wakin, M.: An introduction to compressive sampling. IEEE Signal Process. Mag., **25** (2008), 21–30.

[17] Baraniuk, R.G.; Candès, E.; Nowak, R.; Vetterli, M.: Special section on compressive sampling. IEEE Signal Process. Mag., **25** (2008), 12–101.

[18] Gurbuz, A.C.; McClellan, J.H.; Scott, W.R.: Compressive sensing for GPR imaging. Asilomar Conference on Signals, Systems, and Computers, 2007.

[19] Gurbuz, A.C.; McClellan, J.H.; Scott, W.R.: A compressive sensing data acquisition and imaging method for stepped frequency GPRs. IEEE Trans. Signal Process., **57** (2009), 2640–2650.

[20] Gurbuz, A.C.; McClellan, J.H.; Scott, W.R.: Compressive sensing for subsurface imaging using ground penetrating radars. Signal Process., **89** (2009), 1959–1972.

[21] Yoon, Y.; Amin, M.G.: Imaging of behind the wall targets using wideband beam forming with compressive sensing. 15th Workshop on Statistical Signal Process., 93–96, August 31-September 3 2009.

[22] Turk, A.S.; Keskin, A.K.; Senturk, M.D.: Dielectric loaded TEM horn-fed ridged horn antenna design for ultra wideband ground-penetrating impulse radar. Turkish J. Elect. Eng. Comput. Sci., **23** (2015), 1479–1488.

[23] Turk, A.S.; Ozkan-Bakbak, P.; Durak-Ata, L.; Orhan, M.; Unal, M.: Reconstruction of through-the-wall imaging radar signals by compressive sensing. Signal Processing Symp. (SPS 2015), Poland, 10–12 June 2015.

[24] Grant, M.; Boyd, S.: Matlab software for disciplined convex programming (Web Page and Software) 2008. Available: http://cvxr.com/cvx/

[25] Dogaru, T.; Nguyen, L.; Le, C.: Computer models of the human body signature for sensing through the wall radar applications. ARL-TR-4290, September 2007.

Ahmet Serdar Turk received his B.S. degree from Electronics and Telecommunications Engineering Department of Yildiz Technical University, Istanbul, Turkey in 1996, and the M.S. and Ph.D. degrees from the Gebze Institute of Technology, Kocaeli, Turkey in 1998 and 2001, both in Electronics Engineering, respectively. From 1996 to 1999, he worked as a research assistant in the Electronics Engineering Department of Gebze Institute of Technology, and between 1998 and 2008 he worked as senior researcher in Tubitak Marmara Research Center. He is currently professor with head of the Electronics and Communications Engineering Department of Yildiz Technical University. His research interest are ground penetrating radar, synthetic aperture radar, ultra-wide band antenna design, computational electromagnetic and, remote sensing.

https://doi.org/10.1017/S1759078716000593 Published online by Cambridge University Press

Pınar Ozkan-Bakbak received her B.S. and M.Sc. from Yildiz Technical University, Istanbul, Turkey. She has been working as a Research Assistant since 2005 and attending her Ph.D. in the Electronics and Communications Engineering Department of Yildiz Technical University. Her research interests include optical communication, digital signal processing, and optimization techniques.

Lutfiye Durak-Ata received her B.S., M.S., and Ph.D. degrees all in Electrical Engineering Department of Bilkent University, Ankara, Turkey. She worked in the Statistical Signal Processing Laboratory of Korean Advanced Institute of Science and Technology, KAIST. She worked in the Electronics and Communications Engineering Department of Yildiz Technical University, Istanbul, Turkey between 2005 and 2015. Since September 2015, she has been working in Informatics Institute of Istanbul Technical University, where she is currently an Associate Professor. Her research interests are in time–frequency signal processing, adaptive signal processing, statistical signal processing, and communications theory.

Melek Orhan received the B.S. degree from Yildiz Technical University, Istanbul, Turkey, in 2014 in Electronics and Communications Engineering. She is currently working towards the M.S. degree at the YTU. Her research interests include ground penetrating radar signal processing, and SAR imaging.

Mehmet Unal received his B.Sc. and M.Sc. degrees from Pamukkale University, Denizli, Turkey. He has been working as a research assistant in the Electronics and Communications Engineering Department of Yildiz Technical University since 2010. His research interests include biomedical electromagnetic, optical communication, and radar signal processing.

https://doi.org/10.1017/S1759078716000593 Published online by Cambridge University Press